

P10.15

TWO TORNADIC THUNDERSTORMS IN OSTENSIBLY WEAK DEEP LAYER SHEAR ENVIRONMENTS IN SOUTHEASTERN COLORADO: CYCLIC SUPERCELLS OF 25 MAY (KIOWA COUNTY) AND 31 MAY (BACA COUNTY) 2010

John Monteverdi*, San Francisco State University, San Francisco, CA
Michael Umscheid, National Weather Service, Dodge City, KS
Evan Bookbinder, National Weather Service, Kansas City/Pleasant Hill, MO

1. INTRODUCTION

On 25 May and 31 May 2010, long-lived, cyclic tornadic supercells (Bunkers et al. 2006) occurred in Kiowa and Baca Counties, respectively, in southeastern Colorado. While the occurrence of tornadic supercells in this portion of the country is not unusual climatologically, what ultimately led to our interest in documenting these events was that neither storm developed in a shear environment that conventional wisdom suggested could support long-lived cyclic supercells.

Rotating storms were anticipated on both days, however the weak deep layer shear environments (exemplified by winds initially 10 m s^{-1} or less at 500 mb) suggested that the rotating phase of such storms would be brief because precipitation would overwhelm the updraft areas before storms could take advantage of the low-level shear environment.

In addition, in both cases, initial hodographs showed that ground-relative winds at the top of the 0-3 km layer were very light, despite enormous clockwise loops in the hodographs. Thus, interrogation of ground relative winds in this layer could have lead some forecasters to the conclusion that storms might have insubstantial inflow.

The Kiowa County storms of 25 May produced at least three supercell tornadoes (Fig. 1) as it moved into western Kansas northwest of Tribune (see Table 1). The Baca County storm of 31 May produced two supercell tornadoes near Pritchett and eventually moved on to the southeast producing an additional significant, long-lived, and long track tornado (Fig. 2) along with other shorter-lived tornadoes as the storm moved into the Oklahoma Panhandle (see Table 1).

The authors noted separately some other unusual aspects of the storm development on these two days. The primary author, Monteverdi, documented the Kiowa County storms and noted that initial storm motions deviated almost 100 degrees from the anticipated storm motions computed using classical hodograph analysis techniques (i.e., Bunkers technique).

*Corresponding author address:

Prof. John P. Monteverdi, Dept of Geosciences, San Francisco State University, 1600 Holloway Avenue, San Francisco, 94132; e-mail: montever@sfsu.edu



Figure 1 – Tornado associated with the Kiowa County storm near Towner, CO at around 2155 UTC May 25. Photo by John Monteverdi.



Figure 2 – Tornado associated with the Baca County storm of 31 May near Campo, CO at around 0025 UTC 1 June. Photo by Michael Umscheid.

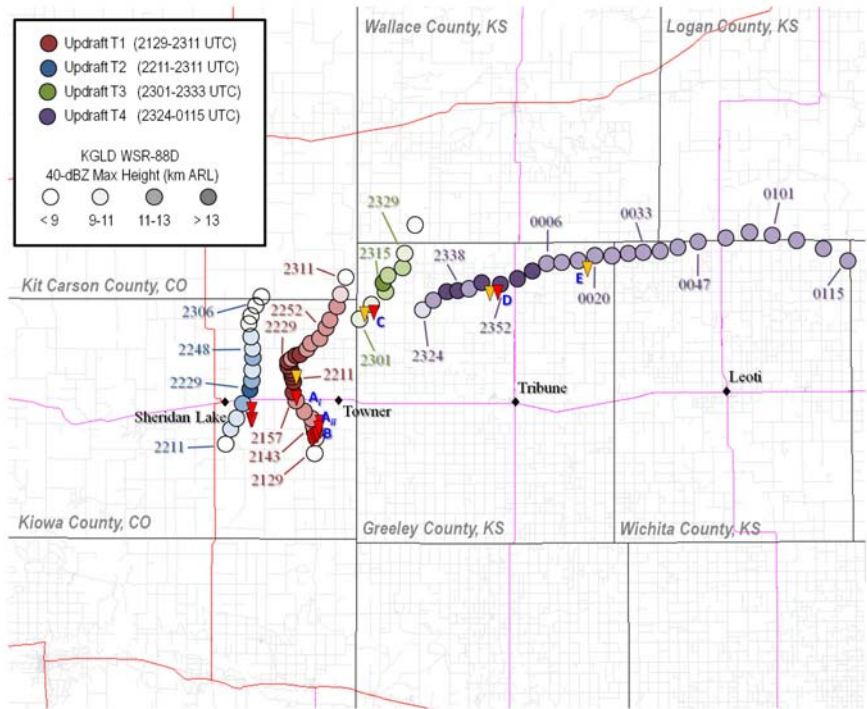


Figure 3 – Locations of tornadoes reported in Storm Data (red triangles) and of other possible tornadoes/funnel clouds (orange triangles) not reported in Storm Data. UTC time stamps on 25 and 26 May 2010. Circles indicate updraft location as determined from analyses of the KGLD radar data, discussed in section 2.

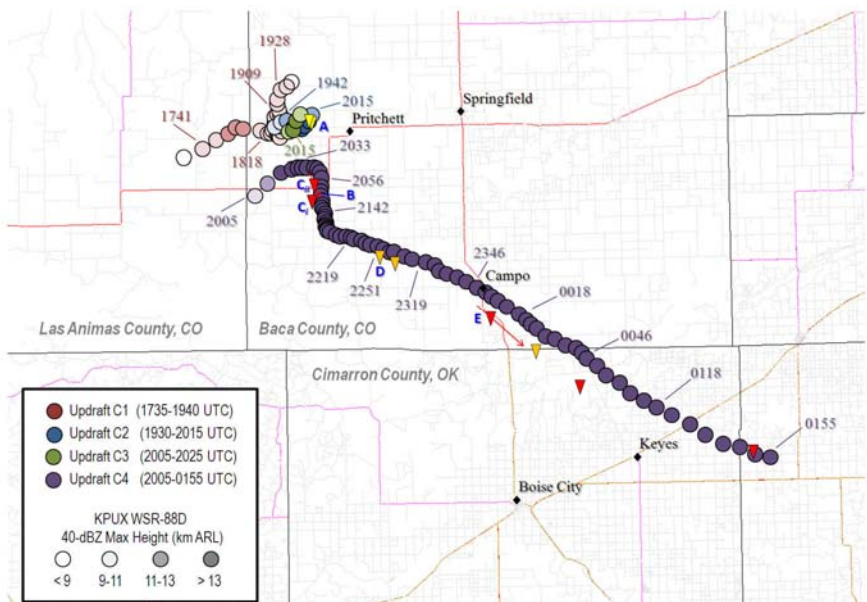


Figure 4 – As in Fig. 3, except for 31 May and 1 June 2010, and KPUX as source of radar data. Yellow triangles show locations of funnel clouds.

Umscheid documented the entire life cycle of the Baca County storm and also noted that storm motion was nearly 90 degrees from the anticipated storm motion for a portion of its life.

It was these observations that led us (a) to consider the hypothesis that the unusual storm motions created storm-relative wind and shear profiles favorable for long-lived tornadic supercells; and (b) to realize that these cases were united not only by similar kinematic environments, but also by the probable fact that the unusual storm motions transformed the risk from minimal to significant that tornadic storms would occur, despite conventional wisdom.

Initially, the authors were separately considering researching the storm they observed, but eventually realized that both events shared some very unusual, but common, characteristics. Besides the kinematic aspects of the storm initiation environments, we both separately noted the importance of updraft interaction with several boundaries in both areas as a source for low level rotation and storm propagation. As a result, we decided to combine our studies into one, stressing the common aspects (but noting the differences).

The authors view this conference presentation as a pilot study. In this manuscript and poster, we seek merely to examine the evidence that our hypothesis has basis, and that there is enough justification to seek a formal publication in the future. Hence, the purpose of this study is to provide a summary of the synoptic and mesoscale environment within which these storms formed. In particular, we seek to examine the thermodynamic and wind shear and aspects of the subsynoptic environment that helped foster initially unusual storm motions that transformed this event to one supportive of briefly rotating, nearly pulse thunderstorms to one that should have been anticipated (in hindsight) to support tornadic supercells.

Sheridan Lake/Towner/Tribune Tornado Times: 25 and 26 May 2010

UTC	Location	County	State	Lat	Lon
2141	3 SW TOWNER	KIOWA	CO	3844	10212
2153	SHERIDAN LAKE	KIOWA	CO	3847	10229
2155	TOWNER	KIOWA	CO	3847	10208
2158	3 SSW SHERIDAN LAKE	KIOWA	CO	3842	10231
2320	4 N TOWNER	KIOWA	CO	3853	10208
2349	9 N TRIBUNE	GREELEY	KS	3860	10178

Pritchett/Campo Tornado Times: 31 May and 1 June 2010

2053	11 SW PRITCHETT	BACA	CO	3726	10300
2103	6 SSW PRITCHETT	BACA	CO	3729	10290
0009	3 S CAMPO	BACA	CO	3706	10258
0059	11 NW KEYES	CIM	OK	3692	10239
0151	4 WNW EVA	TEXAS	OK	3682	10197

Table 1 : Tornado times and locations reported to SPC and logged in Storm Data.

2. STORM EVOLUTION AND HISTORY

A complete analysis of Level-II Weather Surveillance Radar 88 Doppler (WSR-88D Goodland, KS [KGLD] for 25 May; Pueblo, CO [KPUX] for 31 May; Amarillo, TX [KAMA] near the latter stages of 31 May) was conducted for both cases starting from storm initiation and ending around the time each storm either changed convective mode from supercellular to quasi-linear structure, or weakened all together. Figures 3 and 4 show a volume scan by volume scan plot of the primary updraft(s) associated with each storm. At several times during the evolution of both storms, there were concurrent significant updrafts, which can be seen by some overlapping times in the plots on Figures 3 and 4. WSR-88D data was subjectively analyzed using primarily mid-level elevation angles to track significant updrafts. Spatial and temporal continuity was important in the final analysis of the updraft centroids, which are indicated by small shaded circles in Figures 3 and 4. The shading of the circles in these figures represent updraft intensity, and the base reflectivity 40-dBZ maximum height level was used to gauge updraft intensity in this analysis. The authors choose to break down the analysis of the storm structure and evolution into three distinct phases, of which both the Kiowa County storm and Baca County storm each shared some common aspects as well as notable differences.

2.1 Phase 1 – Initiation and non-supercell tornadoes/high-based funnels

The pre-supercell phase of both the Kiowa and Baca County storms had their own unique identity. The Kiowa County storm on 25 May only appeared to be non-supercellular for about the first 30 or 40 minutes of its existence. In the formative stages of the first significant Kiowa County storm updraft (Updraft T1 in Fig. 3 and hereafter “T1”), between 2125 and 2135 UTC (Times hereafter in UTC), the updraft was actually comprised of several embedded updraft pulses extending along a south-southwest to north-northeast orientation, most likely along a quasi-stationary north-south boundary (acting as a dryline as depicted in Fig. 11). It was during this initial updraft strengthening phase that numerous non-supercell (landspout) tornadoes developed to the south-southwest of Towner, CO. Anywhere from eight to ten tornadoes occurred between 2131 and 2203 as documented and photographed by numerous storm chasers, including the primary author, Monteverdi, and reported officially in Storm Data. There were a few times that two or more tornadoes were occurring simultaneously, including an apparent unusual Fujiwhara effect where two nearby tornadoes appeared to orbit around a common center (Fig. 5b). Once T1 became coherent with good temporal continuity, a storm motion could then be determined. The initial updraft motion of T1 was around 164 degrees at 13 kts ($\sim 6.5 \text{ m s}^{-1}$).

The pre-supercell phase of the Baca County storm on 31 May, on the other hand, was much different and more complicated. The duration in time that the Baca

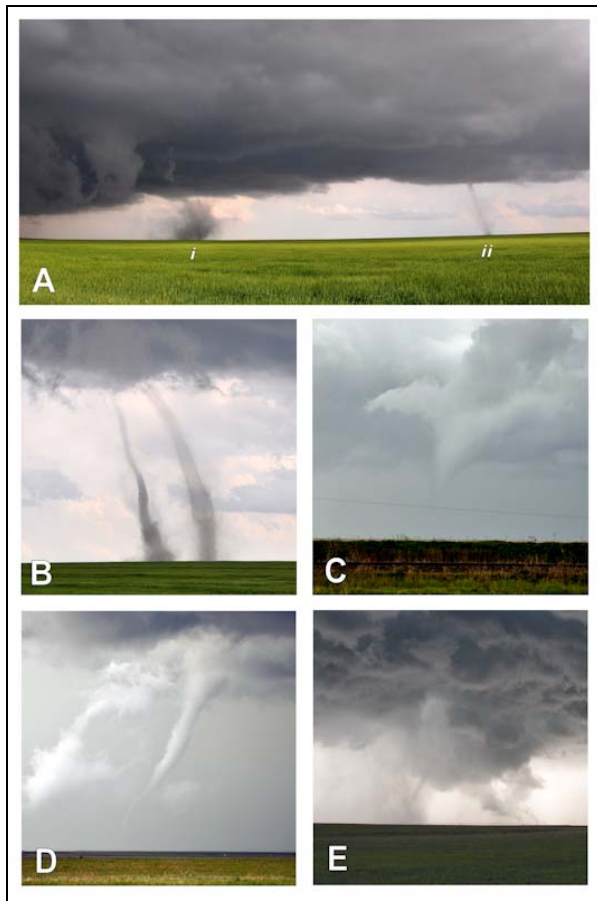


Figure 5 – Sequence of photographs showing tornadoes associated with Kiowa County storm of 25 May. Letters correspond to location of tornadoes mapped in Figure 3. Photos by John Monteverdi.

County storm was non-supercellular was much longer and comprised of several updraft iterations, per WSR-88D data. The first traceable echo marking the beginning of the first significant updraft of the Baca County storm (Updraft C1 in Fig. 4 and hereafter “C1”) was around 1730 just west of the Las Animas-Baca County line. From then on until around 1815 or so, C1 moved slowly from about 262 degrees at 12 kts ($\sim 6 \text{ m s}^{-1}$) into far western Baca County until slowing down considerably by around 1820. C1 appeared to become anchored along a quasi-stationary fine-line that could be discerned in the WSR-88D reflectivity data at 0.5 degrees elevation from 1820 to around 1910. The mid-level echo then drifted north between 1910 and 1940 before diminishing in favor of a new updraft (Updraft C2 in Fig. 4 and hereafter “C2”) about 9 km to the south. Between 1940 and 2010, C2 drifted very slowly to the east-northeast about 7 km west of Pritchett and also became a much taller and more impressive updraft with 45 to 50 dBZ reflectivity echo, reaching nearly 13 km in altitude. The mean updraft motion of C2 was nearly stationary from 1945 until around 2015. While C2 did exhibit some weak rotational signature on radar during this time frame, it was rather broad and weak with mean rotational velocity never exceeding around 30 kts (~ 15

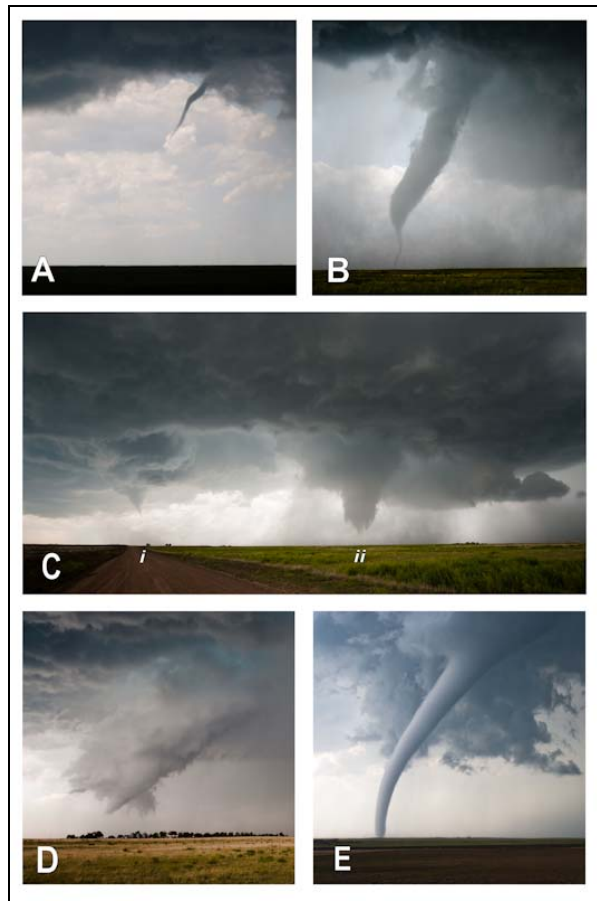


Figure 6 – Sequence of photographs showing funnel clouds and tornadoes associated with Baca County storm of 31 May. Letters correspond to location of tornadoes mapped in Figure 4. Photos by Michael Umscheid.

m s^{-1}). The second author, Umscheid, chased and documented this storm throughout, and photographed two funnel clouds associated with C2. The two funnel clouds occurred at around 1954 and 2002. The second funnel cloud had a more pronounced condensation funnel (Fig. 6a) and may have been marginally supercellular in its development, but the observed rear-flank downdraft clear slot was rather nondescript and not totally obvious. C2 eventually gave way to yet another updraft surge to its immediate west (Updraft C3 in Fig. 4 and hereafter “C3”) by a few kilometers at around 2005, or shortly after the second funnel cloud dissipated in association with C2. By this time, Umscheid was not able to observe the updraft base associated with C3 due to the fact that another updraft (Updraft C4 in Fig. 4 and hereafter “C4”) about 16 km to the southwest was beginning to produce a substantial precipitation core in its forward flank downdraft region at his observing location about 6 km west of Pritchett. C4 grew substantially after 2010 and became the dominant updraft as it initially moved northeast (from 230 degrees), effectively ingesting what was the newly developed and smaller C3 to its north and what was left of C2 a little bit farther to the northeast. A 3-to-1 cell

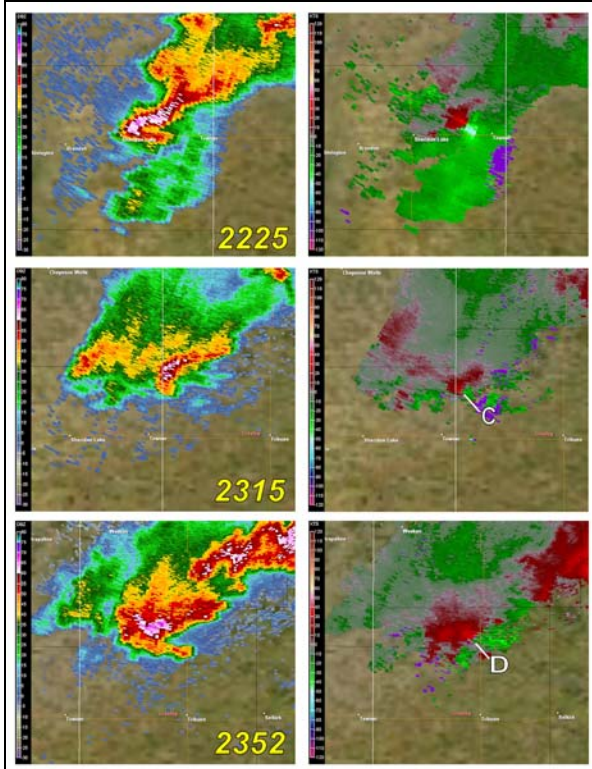


Figure 7 – KGLD WSR-88D base reflectivity (left column) and base velocity (right column) for the 0.5 degree elevation angle at various stages of the Kiowa County storm of 25 May. Times in UTC and letters correspond to photographs of tornadoes in Fig. 5 at the indicated location.

merger took place between 2010 and 2025, and thus marked the beginning of what was to become the long-lived supercell identified as C4.

2.2 Phase 2 – Early supercell tornadoes

The Kiowa County and Baca County storms both transitioned into supercell storms with a deep, persistent rotational velocity signature that was tracked by WSR-88D. After producing the flurry of non-supercell tornadoes, T1 (associated with the Kiowa County storm) showed stronger mid level rotation beginning around 2200 with a marked increase in inbound velocities in the inflow region of the storm, and thus marked the beginning of the supercell phase. Monteverdi photographed a tall tornado with a dramatic translucent dust tube and small condensation funnel at around 2155 approximately 6 km west of Towner (Fig. 1). There may have been supercell processes tied to the genesis of this tornado as this tornado was located north of the flurry of other non-supercell tornado activity farther to the south. This tornado dissipated (“i” in Fig. 5a) a few minutes later while another tornado to its south (which the authors believe was non-supercellular in nature) was still ongoing (“ii” in Fig. 5a). Soon after, as T1 began to interact with an east-west synoptic baroclinic zone, a very dramatic tail cloud formed to the

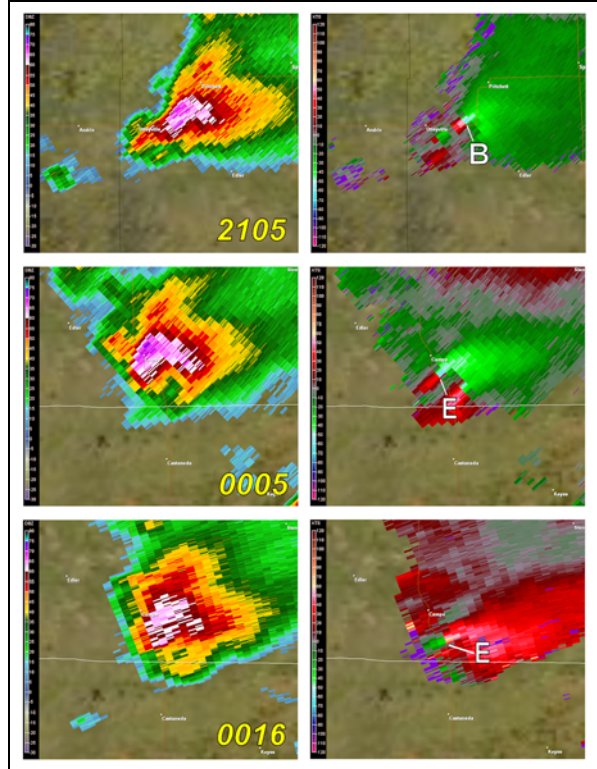


Figure 8 – As in Fig. 7 except KPXX WSR-88D first two rows and KAMA WSR-88D last row at various stages of the Baca County storm of 31 May. Letters correspond to photographs of tornadoes in Fig. 6 at the indicated location.

west-northwest of Towner, and several storm chasers remarked how vigorous the upward vertical motion was with this feature. Several storm chasers claimed to have observed a large tornado sometime during the 2210 to 2225 time frame, however there exist no definitive photographic evidence of such a tornado. The 0.5 degree elevation angle from KGLD at 2225, however, did show a strong rotation couplet with a gate-to-gate (G2G) velocity difference (ΔV) of around 80 kts ($\sim 40 \text{ m s}^{-1}$, top-right panel Fig. 7). This strong G2G shear only lasted a couple of volume scans before weakening as it moved slowly north. Between 2200 and 2300 the storm motion was slightly west of due north, from 160 degrees at around 7 kts ($\sim 3.5 \text{ m s}^{-1}$). During this time frame, there was another updraft (Updraft T2 in Fig. 3 and hereafter “T2”) to the southwest of T1. This updraft may have been responsible for at least a couple of non-supercell tornadoes (as recorded in Storm Data) about 5 km southeast of Sheridan Lake. T1 and T2 became very closely associated with each other between 2215 and 2245 and may have been a contributing factor in allowing T1 to pull to the north-northwest during this time before taking on a storm motion from about 220 to 240 degrees. T1 and T2 both subsequently weakened by 2300 and eventually dissipated as a new updraft developed (Updraft T3 in Fig. 3 and hereafter “T3”) 5km to the southeast of the dissipating T2 (most likely at the triple point of the

forward flank downdraft, rear flank downdraft, and inflow sector). T3 was short-lived, as it could only be tracked by radar data for about 30 minutes. During that time, though, there was a 3-minute tornado about 27 km northwest of Tribune, KS which was photographed by many storm chasers. This tornado was actually comprised of two distinct condensation funnels with the second condensation funnel larger and reaching to the surface (Fig. 5c). The mean storm motion for T3 was from roughly 220 degrees at 12 kts ($\sim 6 \text{ m s}^{-1}$).

C4 associated with the Baca County storm on 25 May began showing supercell structure on radar almost immediately after the absorption of C2 and C3. C4 then began to move sharply to the right, owing to aggressive rear flank tower development feeding the main supercell updraft from the southwest. It is not entirely clear what contributed to such aggressive rear flank tower development from the southwest during the 2030 to 2130 time frame, but it should be noted that 25 to 30 km to the southwest of C4 is the enhanced elevation and terrain that make up the Raton mesas, and terrain induced or enhanced boundaries were likely a major factor in the due-south storm motion through about 2200. During this south-moving phase of C4, a significant (rated EF-2 by National Weather Service), long-lived supercell tornado formed and lasted about 20 minutes. KPIX radar data showed a tornado-vortex signature (TVS; Brown et al. 1978) with G2G delta-V of 90 to 110 kts (~ 45 to 55 m s^{-1}) on several volume scans (top-right panel Fig. 8) between 2100 and 2120 at the 0.5 degree elevation angle, despite KPIX being at a range of 170 km to the storm and sampling at a height of 3 km at the lowest elevation angle (0.5 degrees). Second author Umscheid photographed the entire life cycle of this tornado (Fig. 6b) from a viewing location within the inflow sector looking to the northwest. At around 2110, an additional brief tornado occurred in the anticyclonic shear area ("i" in Fig. 6c) of the rear-flank downdraft about 2 km to the south-southwest of the larger cyclonic tornado ("ii" in Fig. 6c). After the cyclonic tornado dissipated, C4 continued to move from about 355 degrees at around 5 kts ($\sim 2.5 \text{ m s}^{-1}$) or less through 2210 when the supercell began to move more to the southeast from 300 degrees.

2.3 Phase 3 – Late supercell tornadoes

By this final phase in both the Kiowa County and Baca County storms, the supercell was well-established and moving in a relatively constant forward motion, closer to predicted storm motion using Bunkers method, and without much deviation until the storm's end as a supercell. The final phase of the Kiowa County storm (which by this time was east of Kiowa County and into far west-central Kansas) began around 2330 with the emergence of primary updraft T4. From this point forward until about 0115, the supercell was analyzed as a single primary updraft T4 based on radar data. The temporal continuity remained strong during this nearly two-hour phase without any additional significant updraft dissipation and redevelopment (either in the inflow region or otherwise). The only substantiated tornado

associated with T4 developed 16 km north-northwest of Tribune about 30 minutes after the genesis of this particular updraft. This tornado was also thoroughly documented by numerous storm chasers, including primary author MonteVerdi (Fig. 5d). This was a weak tornado as well and fairly short-lived lasting only a minute or two. Per analysis of KGLD radar data, an outflow boundary from other severe storms to the northeast of T4 appeared to begin to undercut the Kiowa storm by as early as 0010. Despite this, another weak probable tornado was documented by several storm chasers, including MonteVerdi, at around 0020 about 23 km northeast of Tribune (Fig. 5e). Due to darkness and the fact the storm was now substantially undercut by outflow, many storm chasers no longer pursued the Kiowa County storm after the last documented probable tornado. For the sake of brevity, the Kiowa County storm was not mapped in Figure 3 after 0115, however interrogation of KGLD radar data continued to support supercell structure, particularly in mid-level velocity data, through 0200. As a result, the evidence presented here suggests that the supercell phase of the Kiowa County storm lasted at least four hours, meeting the "long-lived supercell" criteria (Bunkers et al. 2006).

The Baca County storm of 31 May produced one more long-lived tornado (in addition to several smaller short-lived tornadoes and substantial funnels) in the final, and longer phase of this storm. On radar, C4 began to move to the southeast (from about 300 degrees) around 2210. C4 cycled through a significant occlusion, producing a visually impressive wall cloud and eventual laminar funnel cloud at around 2300, per observations and photographs by Umscheid (Fig. 6d). There may have been a weak tornado associated with this funnel, however ground contact in the form of a small debris cloud could not be observed. This area eventually wrapped up in rain and at 2310, a suspect large, bowl-shaped laminar cloud feature emerged amidst the semi-transparent rain core. Again, a tornado may have occurred here, but ground contact could never be discerned. The storm would be non-tornadic again until 0005 when the genesis of the second long-lived tornado associated with the Baca County storm occurred about 5 km south of Campo, CO. This tornado was highly visible and well-documented by numerous storm chasers, including Umscheid (Figs. 2 and 6e). Like the first long-lived tornado three hours prior, an impressive G2G delta-V signature was observed both by KPIX and KAMA (Fig. 8) as these radars were equidistant to the Baca County storm by this time. The tornado moved southeast until finally dissipating about twenty minutes later around 0025. Another short-lived tornado occurred about 5 minutes later, most likely just south of the Oklahoma-Colorado state border, which the authors found undocumented in Storm Data. This tornado occurred between 0030 and 0036 and was wrapped in rain and hail for most of its life. Yet another tornado occurred around 0100 as C4 continued its southeast track, and one final tornado was reported in Storm Data at 0151 shortly before the storm weakened. All told, a total of at least six supercell tornadoes were

produced by the Baca County storm of 31 May. Like the Kiowa County storm of 25 May, the evidence presented in this study also suggests that the Baca County storm lasted at least four hours as a supercell storm, meeting the “long-lived supercell” criteria (Bunkers et al. 2006).

3. SYNOPTIC, THERMODYNAMIC AND KINEMATIC CONTROLS

3.1 Synoptic Scale Environment

Several key features in the synoptic-scale environment were similar for both the Kiowa County and Baca County storms. Middle and upper tropospheric flow over the central Great Plains was anemic in both cases. These storms occurred during a week-long period characterized by a major anchor trough in the southern portions of western Canada into the northern Great Basin (not shown). Strongest flow in the middle and upper troposphere extended generally across Idaho, Montana and into eastern Wyoming and then northeastward, with only a fringe of 12 to 17 m s⁻¹ winds impinging on the western High Plains of Colorado, extreme western Kansas and the northwestern Oklahoma and Texas Panhandles. Southwesterly flow characterized all levels of the troposphere above 850 mb over the Great Plains on 25 May and zonal flow on 31 May.

In both cases, weak upper tropospheric disturbances were upstream of the storm genesis regions, and brought weak upward vertical motion fields in the mid troposphere over both areas during the time of thunderstorm genesis (Fig. 9a, b). On 25 May (Fig. 9a), the upward vertical motion field in the lower mid-troposphere had overspread eastern Colorado by 18 UTC. This gentle lofting undoubtedly contributed to destabilization that aided storm initiation along and just west of the Kansas border from Sterling southward. On the other hand, the vertical motion field associated with the progressing wave on 31 May (Fig. 9b) was just entering the area at the time of storm initiation. The vertical motion field was complicated by the impact of the mountains.

The surface pressure falls associated with the disturbances in the mid and upper troposphere brought weak cyclogenesis to east-central Colorado on 25 May and in extreme southeastern Colorado on 31 May (Fig. 10a, b). Fig. 10a and 10b should be compared with the composite surface subsynoptic analyses (overlain with the visible satellite imagery) for 2000 UTC 25 May (Fig. 11) and 2000 UTC 31 May (Fig. 12).

The Kiowa County storms formed along and just south of a true triple-point intersection of warm front, dry line and outflow boundary evident both in the surface subsynoptic analysis (Fig. 11) and on the objectively contoured isotherm analysis from the NAM, given as Fig. 9a. We believe that solenoidal circulation associated with the outflow boundary was tilted into the updraft of the Kiowa County storms and contributed to the development of low level rotation and shear values not evident in the shear environment as deduced from hodograph analyses (discussed in the next section).

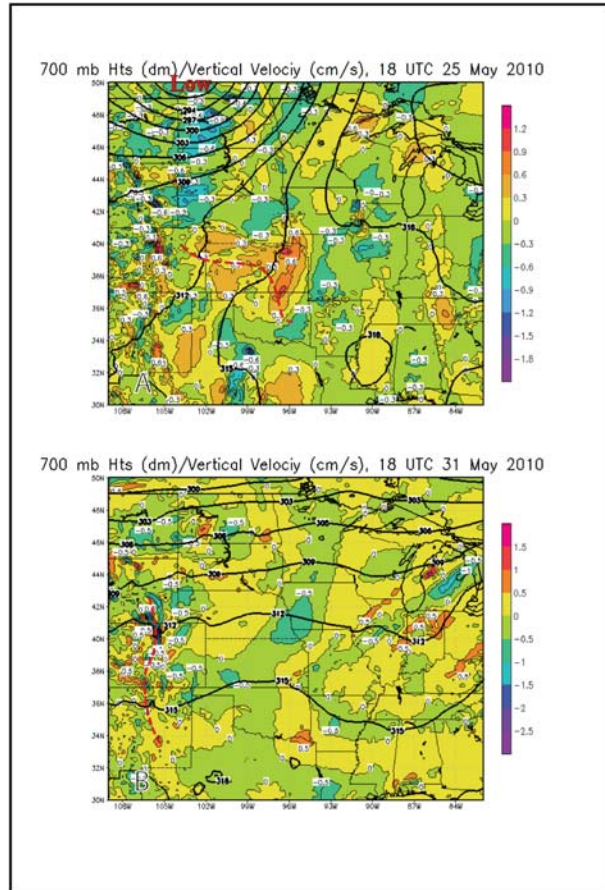


Figure 9 – North American Model (NAM) Reanalyses 1800 UTC (a) 25 May 2010 and (b) 31 May 2010 showing 700 mb heights (dm) and vertical velocity (cm s⁻¹). Dashed red lines represent the axes of weak disturbances progressing eastward and evident in the vorticity field (not shown) at higher levels and enhanced cyclonic curvature at 700 mb.

Such boundaries have been identified as key players in many significant supercell tornado outbreaks (see, e.g., Markowski et al. 1998 and Rasmussen et al. 2000).

We also believe that the storm motion towards the northwest for the first and second Kiowa County storms in their early stages of development, and before they processed through the supercell cascade, had another effect. It was during these early stages that at least five landspout tornadoes were documented near Towner and Sheridan Lake, Colorado. The storm motions during that period were tangent to the intersecting warm frontal boundary, effectively providing a source of horizontal rotation that was tilted and stretched, we believe, into the rapidly developing ascending towers (but before mesocyclones developed).

The Baca County storms formed in a much more complicated subsynoptic environment. The subsynoptic analysis given in Fig. 12 shows that the storm’s updraft

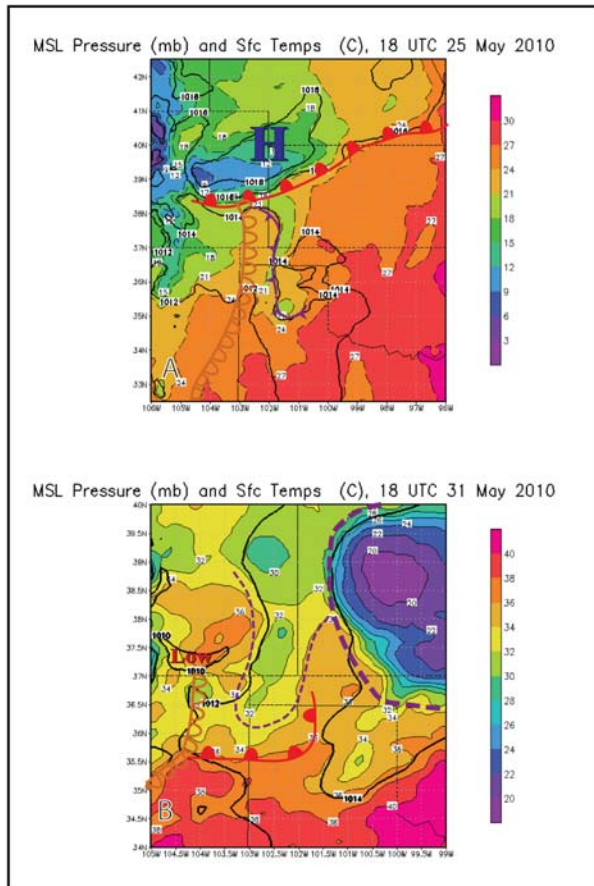


Figure 10 – North American Model (NAM) Reanalyses 1800 UTC (a) 25 May 2010 and (b) 31 May 2010 showing sea level pressure (mb) and temperature (C).

was found in a relatively narrow slot between the dry line to the west, and a boundary, which might have been an outflow boundary¹. The boundary analysis in Fig. 12 was substantiated in the objectively drawn isotherms shown in Fig. 9b. The pool of cool air in extreme southeastern Colorado is clearly visible in this analysis.

As the day progressed, the true warm front to the south advanced northward and joined with the quasi-outflow boundary, producing a much more significant baroclinic zone. The second Baca County storm (and the first to produce supercell tornadoes) moved due south along this boundary. Like the Kiowa County storms, such storm motion had the effect of moving the updraft southward along the boundary, allowing it to ingest the baroclinically-generated vorticity. As in the case of the Kiowa County storms, we believe that this ingestion augmented the low level rotation and shear to larger values than indicated in the hodograph analysis (in the next section). It is also interesting to note that the boundary may have played a role in the generation of high-based funnels in Phase 1 of the Baca County storm, just as the boundaries undoubtedly played a role

¹ The authors have examined the radar information for the previous 24 hours and did not find evidence of any thunderstorms that might have produced an outflow boundary.

in the generation of five or more significant non-mesocyclone (landspout) tornadoes during Phase 1 of the Kiowa County storms.

3.2 Thermodynamic Environment

The synoptic and subsynoptic environments also “set the stage” for adequate thermodynamics for both storms. Analysis of the KAMA and KDDC 12 UTC soundings for May 25 and May 31 (not given) show a “loaded gun” sounding structure, with the edge of the “breakable” cap at around a 700 mb temperature of 8 °C on 25 May and 10 °C on 31 May. The temperature analyses given in Fig. 13 a, b show that the area from the Oklahoma Panhandle northward had 700 mb temperatures <8 °C on 25 May, and the area from the Oklahoma Panhandle northward had 700 mb temperatures <10 °C on 31 May. The surface based Convective Available Potential Energy (sbCAPE) fields are given in Fig. 14a,b and show narrow tongues of moderate to high sbCAPE (>1500 J/kg on 25 May and >2400 J/kg on 31 May) extending (a) between the dry line and the outflow boundary curling back to the warm front on May 25 and (b) between the dryline and the quasi-outflow boundary on 31 May. Thus, the region with “breakable cap” and adequate CAPE really was small on both days, a narrow rectangle that extended from the warm front south to the Oklahoma Panhandle along the Kansas-Colorado border on 25 May and, essentially, just southeastern Colorado and the adjacent Oklahoma Panhandle on 31 May.

Storm development was rapid in the two relatively small areas with no convective inhibition by late morning. On 25 May, storms erupted along a line from the Oklahoma Panhandle just southwest of Elkhart, KS in the region with the highest sbCAPE, and then northward along the Colorado-Kansas border to the aforementioned triple point intersection (Fig. 15). On 31 May, storm initiation took place in the higher terrain near the Las Animas-Baca County line and with subsequent storm initiation further east and then south (Fig. 16).

3.3 Kinematic/Shear Environment

Meteorologists assessing the risk for tornadic convection on the afternoons of 25 May and 31 May had access to a number of differing diagnostic and forecasting products. We remind the reader that in this pilot study we seek only to discover what might have been assessed in forecasting decisions for the day. Thus, although the 0000 UTC soundings and hodographs for the conventional sounding sites would have been closer in time to the actual tornado events, these verification soundings and hodographs, of course, would not be available to forecasters in the morning. For this study, we examine only the wind shear environments assessed from the morning radiosonde launches and Dodge City (KDDC) and at Amarillo (KAMA) and not the forecast soundings and hodographs from any of the numerical models (to put a limit on the scope of this initial study). We are not examining the

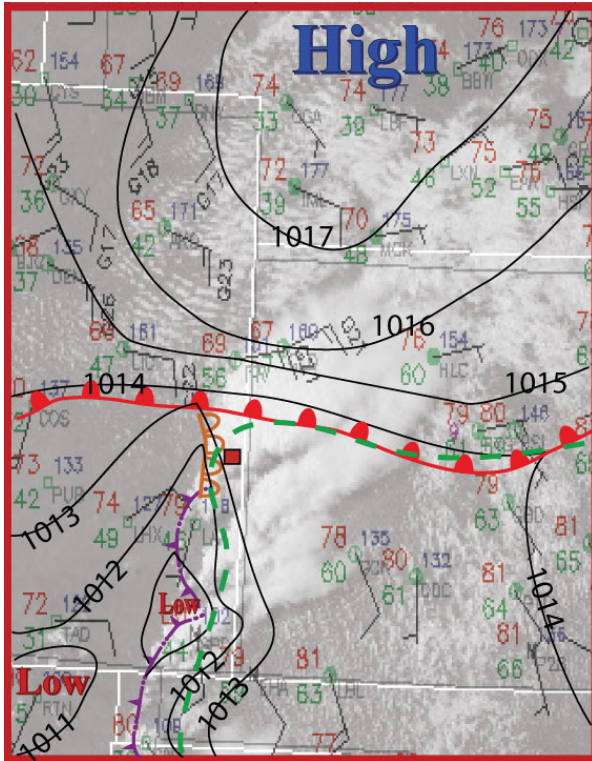


Figure 11 – Overlay of visible satellite imagery at 20 UTC 25 May 2010 on a surface subsynoptic analysis. Square locates approximate position of the Kiowa County storm’s updraft at the time. Green dashed line shows the 60F isodrosotherm. The Kiowa County tornadic storms occurred at a “triple point” intersection of a quasi-stationary warm front, dry line and outflow boundary from more mature storms to the north and south.

thermodynamics of the morning or afternoon soundings because there was no disagreement about initiation in either area, nor was any disagreement that sbCAPE values would be moderate to strong.

What was an issue, evident in the Area Forecast Discussions from National Weather Service Forecast Offices and SPC Convective Outlooks, was whether vertical wind shear through the deep layer was sufficient enough to allow long-lived storms. For the 25 May event, the hodograph (Fig. 17a) plotted for the KDDC radiosonde launch provides a good illustration of the issues.

The 1200 UTC wind profile showed the following: (a) weak ground-relative winds in the middle and upper troposphere, mostly less than 12 m s^{-1} ; (b) weak ground-relative winds even in the lowest layers, with several of the significant levels showing winds $< 4 \text{ m s}^{-1}$; and (c) an extremely large clockwise loop in the lowest 3 km above ground level (AGL). A sampling of the discussions from WFOs and SPC indicated that the fact that clockwise loop suggested rotating storms (with the implied large values of Storm Relative Helicity (SREH) $> 150 \text{ J/kg}$), factors (a) and (b) argued that updrafts would be disorganized and/or precipitation would be

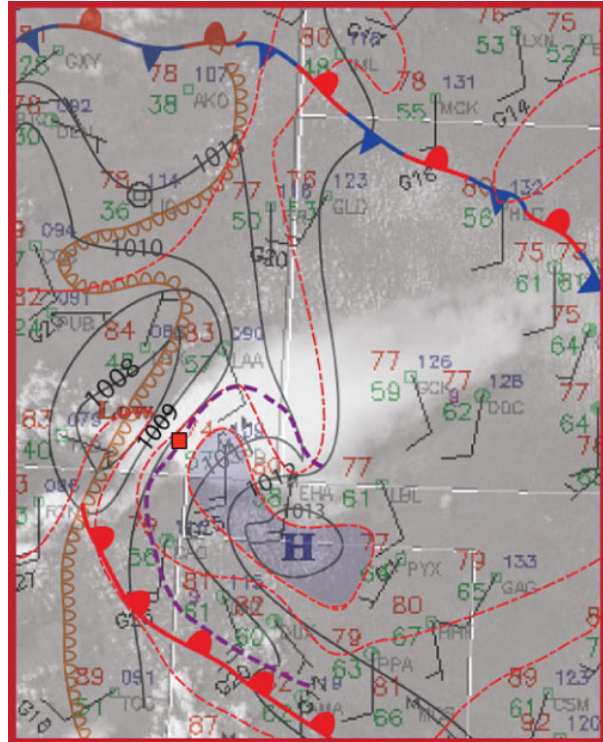


Figure 12 – Overlay of visible satellite imagery at 20 UTC 31 May 2010 on a surface subsynoptic analysis. Square locates approximate position of the Baca County storm’s updraft at the time. Blue shading represents the center of a relatively cold air mass (dashed red lines are isotherms) over the Oklahoma Panhandle whose source is unclear, with the dashed purple line indicating a boundary, effectively an outflow boundary. The Baca County storm formed in the slot between the dry line and this pseudo-outflow boundary, east of the developing surface low pressure area.

quickly ingested into developing mesocyclones, effectively “choking” off the potential for storms to progress through the supercell cascade. The hodograph (Fig. 17a) contains a large anticyclonic loop from 0-3 km. Such a large loop is associated with dynamic pressure forces creating strongly deviant right moving supercells, often associated with mesocyclone tornadoes (Rotunno and Kemp 1985).

Similar issues were evident in the analysis of the 1200 UTC 31 May KAMA hodograph, used as an approximation for the storm initiation environment for the northern Texas Panhandle into southeastern Colorado. In this case (Fig. 18a), the clockwise loop was extremely large, but the anemic flow in the middle and upper troposphere was very obvious, as was the negligible ground-relative flow at lower levels.

We believe that forecasters may have been biased by the products normally posted on websites and conventional wisdom into improper assessment of the shear and kinematic environments for both storms. In particular, we believe the following issues led to misforecasts: (a) use of the popular “bulk shear” in the 0-6 km layer instead of positive (or total) shear to

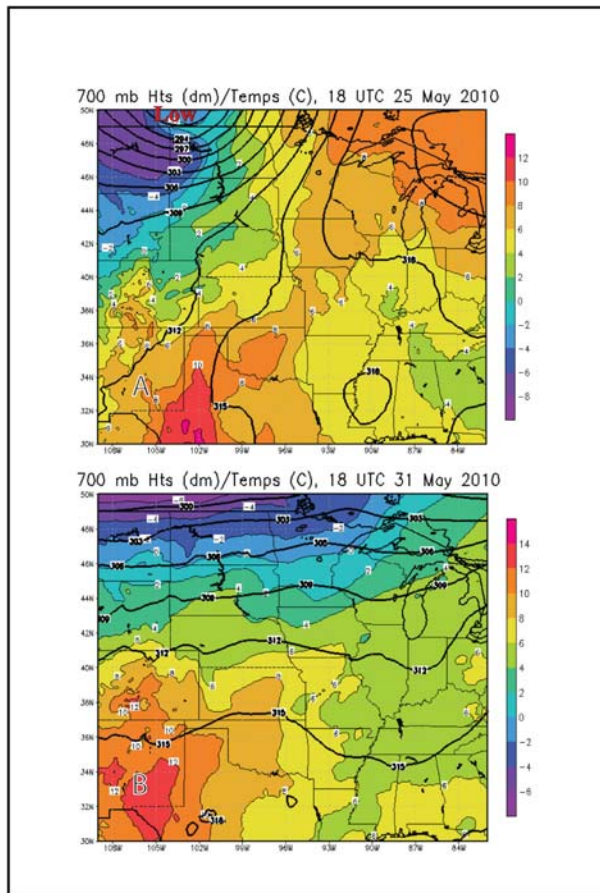


Figure 13 – North American Model (NAM) Reanalyses 1800 UTC (a) 25 May 2010 and (b) 31 May 2010 showing 700 mb heights (dm) and temperatures (C).

assess both the degree to which storms might be long lived (and not suppressed by precipitation and the development of helical updrafts); (b) use of the 500 mb winds as a quick estimate of “bulk shear” in the 0-6 km layer; and, (c) the use of popular algorithms, including the widely-used Bunkers technique (Bunkers et al. 2000), to assess potential storm motions of right-moving supercells.

To help clarify these issues we have listed common shear and kinematic parameters frequently used in severe weather forecasting in Table 2. Next to each parameter we list the values commonly used (or referred to in the literature) to assess either storm longevity, the development of mid-level rotation and/or, the development of low level rotation, with the information structured from top to bottom in the table to mimic the supercell cascade (in which storms must persist in a properly sheared environment for a substantial time, then mid-level rotation develops, with the concomitant development of a radar hook, and then rear flank downdrafts (RFD) can interact with favorable low level shear to produce low level rotation antecedent to tornadogenesis).

In Table 2 we seek to clarify the nature of these parameters and how they influenced forecasting decisions or impressions near the time of first

tornadogenesis, in the case of 25 May, for the first Towner supercell tornado (labeled A1 on Fig. 3) and, in the case of 31 May, for the first Campo tornado (labeled C1 on Fig. 4). On the far right hand columns in Table 2 we list the values of the parameters for the forecast Bunkers storm motion, with the values of the parameters for the actual storm motions as determined from the radar analyses given in Section 2 above. The color coding is as follows: red cells indicate that values are unfavorable either for engendering a long-lived updraft, or the development of rotation at the respective levels, yellow means marginally favorable, and green indicates values exceeding those considered to be favorable for development of sustained rotation.

The values in this Table we believe illustrate the issues. Using conventional wisdom, the mid and upper tropospheric flow simply would not have been favorable for sustained rotating convection. Likewise, most of the storm-relative parameters at anvil-level were also unfavorable for the forecast Bunkers storm motion. In addition, those parameters that are independent of storm motion stayed unfavorable even when the authors input the actual quite deviate storm motion into the calculations.

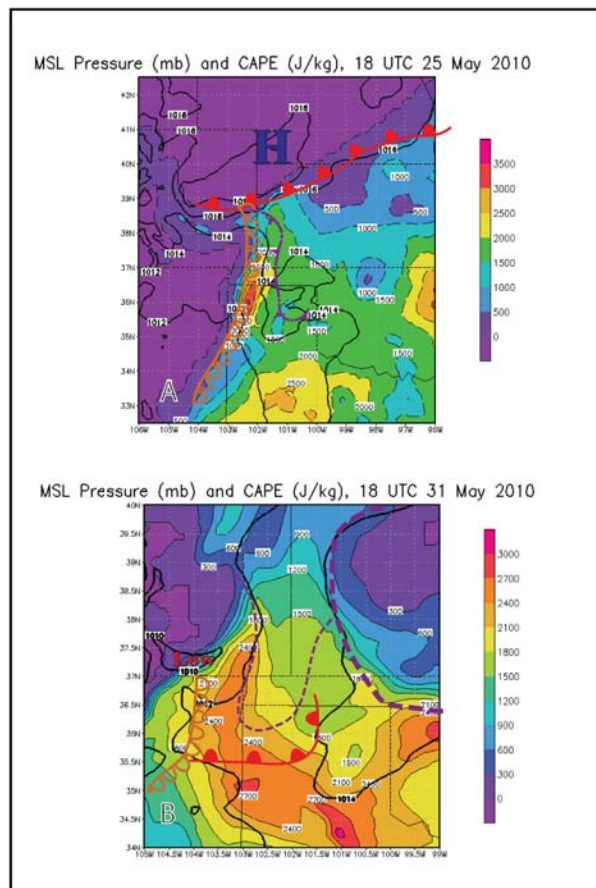


Figure 14 – North American Model (NAM) Reanalyses 1800 UTC (a) 25 May 2010 and (b) 31 May 2010 showing sea level pressure (mb) and sbCAPE, as discussed in text.

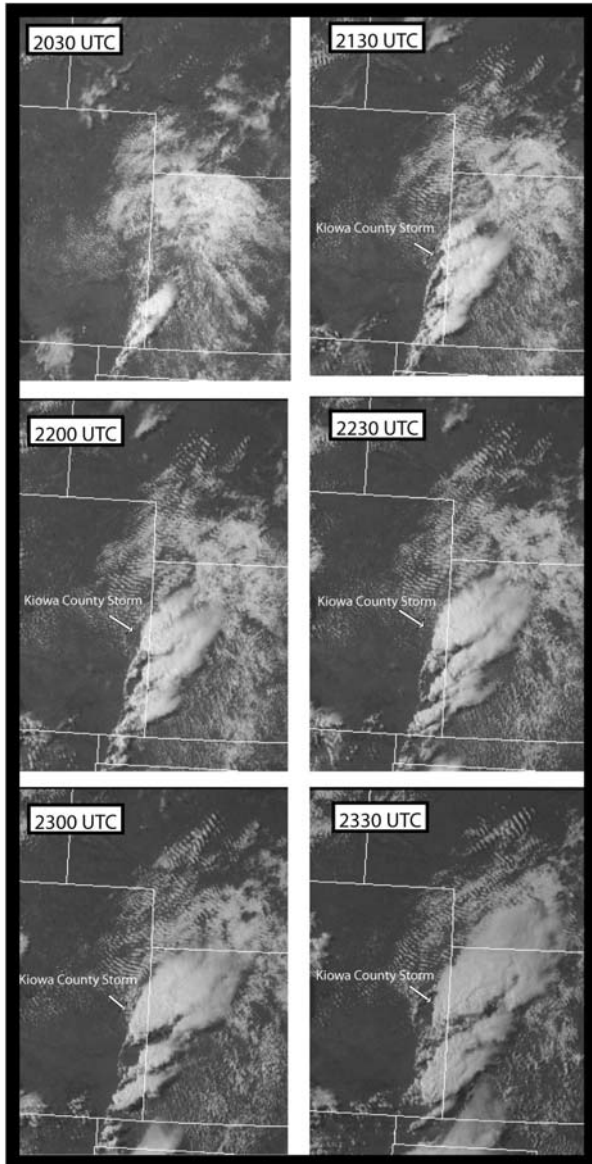


Figure 15. Sequence of visible satellite images showing the development of the storms in eastern Colorado on 25 May. The Kiowa County storm is indicated.

Yet most of the low level parameters suggestive of rotation development were quite favorable. As pointed out above, the issue on both of these days was whether deep layer shear would be supportive of sustained convection with mid-level rotation, and preventing precipitation from overwhelming the updrafts. Clearly, the values of those parameters using the Bunkers storm motion were unfavorable, but were quite favorable for the actual storm motion. The conclusion to be had here is that the use of the Bunkers storm motion would lead forecasters to underestimate the risk that long-lived storms with persistent rotation would occur.

Several other issues emerge when looking at the values in the first two rows of Table 2. First, the 500 mb winds are definitely not indicative of storm-relative flow

or deep layer shear in this region, especially since the 6 km AGL is nearly at the 400 mb level in this portion of the Plains. Thus, the 500 mb winds will usually be less than the 400 mb winds, and lead to an underestimate of the deep layer shear, in this “quick and dirty” method of assessing such shear. Second, the actual ground-relative winds simply do not assess storm relative shear and wind flow, which is really the important issue when deciding whether precipitation will be ingested into the updraft and suppress the storm.

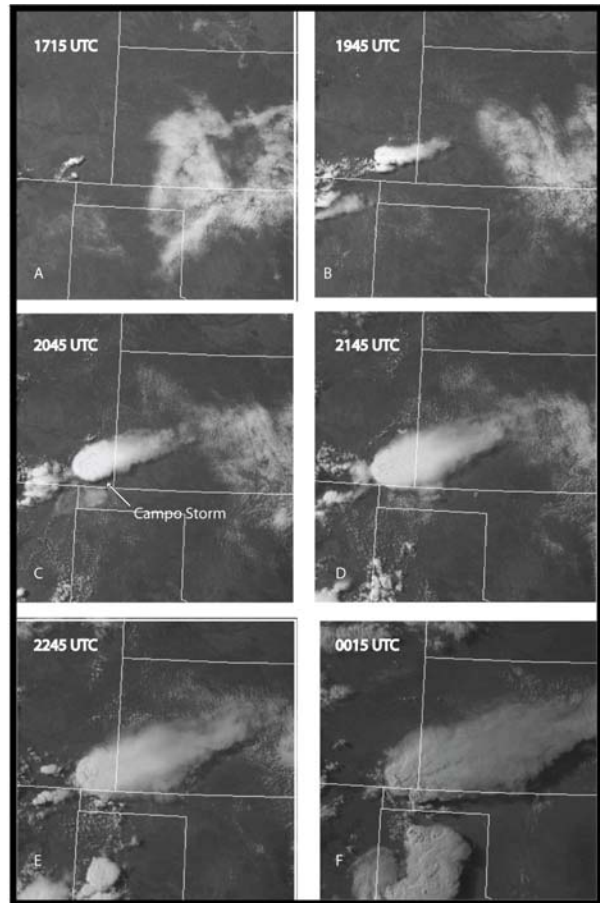


Figure 16. Sequence of visible satellite images showing the development of the storms in southeastern Colorado on 31 May. The Baca County storm (more specifically, Updraft C4 in Fig. 4) is indicated in panel C.

Another major issue centers on the popular use of the “bulk shear” to assess the shear across various layers. The use of this, unfortunately, has spread across the severe storms community and is institutionalized by the use of these values on the SPC website “Mesoanalysis Page”. The comparative information often used to establish thresholds comes from the work of Weisman and Klemp (1986), who showed that supercells are favored with certain values of deep layer shear. The problem is that Weisman and Klemp used total shear, not bulk shear. Total shear is

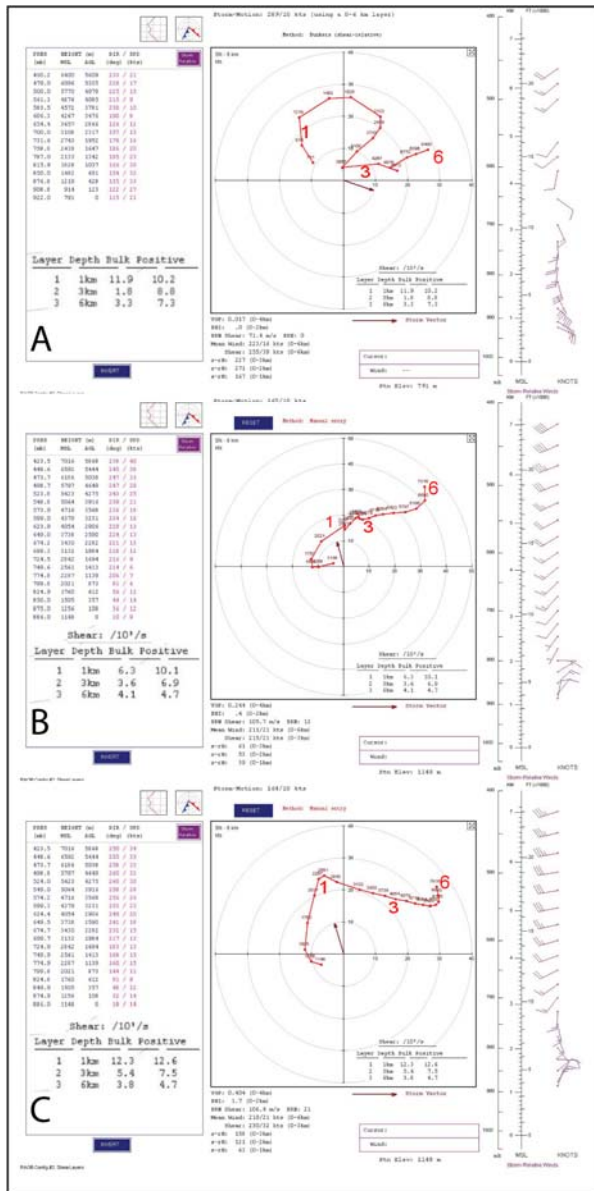


Figure 17. (a) Hodograph of wind information from the 12 UTC 25 May 2010 KDDC radiosonde launch with the estimated storm motion vector (using the Bunkers technique) shown in red. (b) RUC13 hodograph for a grid point near Towner, CO for 2000 UTC 25 May 2010 with the actual storm motion (as inferred from analyses of the radar information) shown in red. (c) As in (b) except for 0000 UTC 26 May 2010. Winds plotted on right margins of each hodograph, and shown in red on the tabular information shown on left margins of each hodograph, represent the storm relative flow for the storm motion vector shown on each hodograph.

the sum of the lengths of the shear vectors from layer to layer – usually very small (i.e. 10 to 25 mb) – and is largely dependent on the vertical resolution of the dataset being analyzed. For a straight hodograph, bulk shear and total shear are identical. For a strongly curved hodograph, total shear will be much larger than the bulk shear over the same layers. Put baldly, bulk shear estimates can grossly underestimate the actual shear environment a convective storm can develop and evolve in.

Finally, on this issue, deviate “right-moving” supercell storms have been shown to relate to the “positive shear” in the hodograph. This is closely related to storm relative helicity and is obtained by summing the shear magnitudes of those vectors that veer (turn clockwise with height) or are neutral (unidirectional). Positive [negative] shear is a measure of the dynamic forces that contribute to right [left] deviate motion. In vertical wind profiles with similar bulk shear magnitude over a specific layer (i.e. 0-3 km AGL), positive shear, will be much larger for a curved hodograph than for a straight hodograph. This is well illustrated in Table 2 by the entries for positive shear, that are included here not because forecasters had access to them, but to show that if they did have access, the risk for tornadic convection may have been better assessed on this day.

A remarkable feature of both hodographs (Figs.17a and 18a) is the intense directional low level shear suggested by the anticyclonic loop, with a strong kink between 1 and 2 km. Such a kink was observed in the VAD-derived hodographs in Oklahoma on the day of the 3 May 1999 tornadic supercell outbreak (Thompson and Edwards 2000).

The last significant issue centers on the forecast storm motion that severe weather meteorologists may have used when estimating initial storm movement vectors. While the Bunkers technique works extremely well for traditionally shaped hodographs, the authors believe that the excessively large anticyclonic (clockwise) loops in the lower levels, found in Figs. 17a and 18a, led to incorrectly forecast storm motions. Since the Bunkers technique heavily depends upon winds in at the steering levels, which were relatively weak in these cases anyway, the forecast storm motions were biased away the deviations that would have been dominant due to the strong directional shear in the low level environment.

As a quick pilot study, the authors changed the shear layers over which the Bunkers forecast technique is evaluated, and essentially made the low level shear the more dominant effect in the expression. The forecast storm motions then more resembled the actual storm motions that occurred for the phases of the storm development (shown in in Figs. 3 and 4) in which the storms not only had strongly deviate motion relative to the hodograph, but had motion far different than forecast by the Bunkers technique.

A final ingredient to the low level rotation would be the rotation “ingested” into the updraft if it moved over a boundary. As mentioned in Section 3.2 above, boundaries were certainly present on both days, and

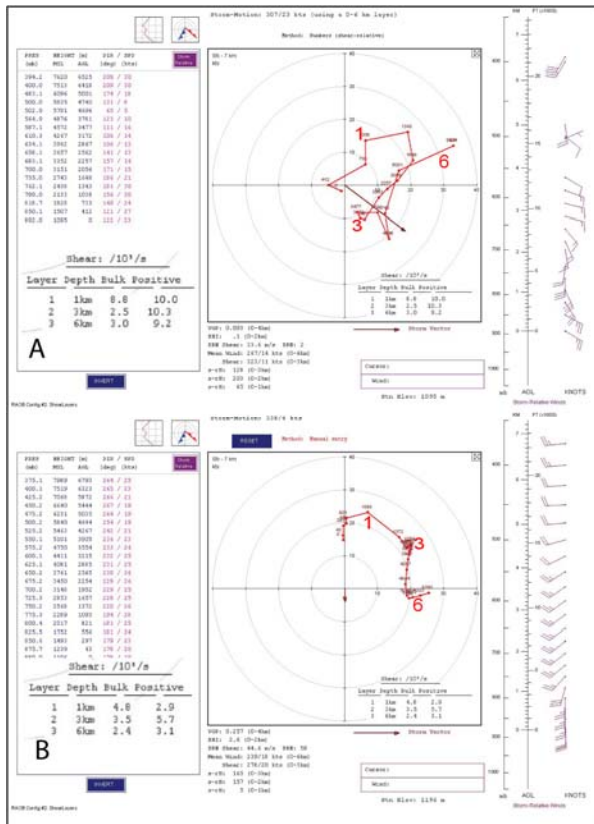


Figure 18. (a) Hodograph of wind information from the 12 UTC 31 May 2010 KAMA radiosonde launch with the estimated storm motion vector (using the Bunkers technique) shown in red. (b) RUC13 hodograph for a grid point near Campo, CO for 2000 UTC 25 May 2010 with the actual storm motion (as inferred from analyses of the radar information) shown in red. Winds plotted on right margins of each hodograph, and shown in red on the tabular information shown on left margins of each hodograph, represent the storm relative flow for the storm motion vector shown on each hodograph.

these boundaries were quite strong. In fact, the boundaries themselves might have strongly affected storm motions.

Also, clearly, if the ingestion of baroclinically-induced vorticity associated with these boundaries was “added” to the ambient vorticity present because of the storm-relative shear for the actual storm motion (the far right hand column of Table 1) then it is a fair assumption that the values in the bottom of the far right hand column for both storms would have been “screaming” the risk of tornadic supercells on this day. Rasmussen et al. (2000) found similar values along boundaries in VORTEX-1, and presented a case study example of a non-tornadic supercell becoming tornadic when it intercepted and “ingested” such boundaries in the Texas Panhandle in 1995.

The authors realize that use of the morning hodograph in this manner is also a mistake. Clearly, the afternoon hodograph might not resemble the morning hodograph at all, so making too many judgments on the

Sheridan Lake Storm: 12 UTC KDDC Hodograph			
Initial Storm Ventilation and Mesocyclone Formation		Storm Motions: Bunkers / Actual	
		289/10 knts	164/13 kts
<i>Conventional Wisdom</i>			
500 mb Winds	> 30 kts	21 knots	21 knots
6 km Winds	> 30 kts	24 knots	24 knots
<i>Refereed Literature</i>			
0-6 km Positive Shear	> 5 X 10 ⁻³ s ⁻¹	7.3 X 10 ⁻³	7.3 X 10 ⁻³
0-6 km Bulk Shear**	> 4 X 10 ⁻³ s ⁻¹	1.72 X 10 ⁻³	1.72 X 10 ⁻³
4-6 km sr Flow	> 15 knots	12 kts	22 kts
6-9 km sr Flow	41-60 knots	48 kts	44 kts
Development of Low Level Rotation/ Mesocyclone Development			
<i>Refereed Literature</i>			
0-3 km Positive Shear	3 X 10 ⁻³ s ⁻¹	8.8 X 10 ⁻³	8.8 X 10 ⁻³
0-3 km Bulk Shear	2 X 10 ⁻³ s ⁻¹	1.8 X 10 ⁻³	1.8 X 10 ⁻³
0-3 km SREH	150-250 m ² /s ²	227 m ² /s ²	215 m ² /s ²
0-1 km SREH	~100 m ² /s ²	167 m ² /s ²	100 m ² /s ²
0-1 km Positive Shear	> 10 X 10 ⁻³ s ⁻¹	10.2 X 10 ⁻³	10.2 X 10 ⁻³
0-1 km Bulk Shear	> 8 X 10 ⁻² s ⁻¹	11.9 X 10 ⁻³	11.9 X 10 ⁻³
Campo Storm: 12 UTC KAMA Hodograph			
Initial Storm Ventilation and Mesocyclone Formation		Storm Motions: Bunkers / Actual	
		294/10knts	360/5 kts
<i>Conventional Wisdom</i>			
500 mb Winds	> 30 kts	15 knots	15 knots
6 km Winds	> 30 kts	30 knots	30 knots
<i>Refereed Literature</i>			
0-6 km Positive Shear	> 5 X 10 ⁻³ s ⁻¹	9.2 X 10 ⁻³	9.2 X 10 ⁻³
0-6 km Bulk Shear**	> 4 X 10 ⁻³ s ⁻¹	3.3 X 10 ⁻³	3.3 X 10 ⁻³
4-6 km sr Flow	> 15 knots	10 kts	22 kts
6-9 km sr Flow	41-60 knots	29 kts	41 kts
Development of Low Level Rotation/ Mesocyclone Development			
<i>Refereed Literature</i>			
0-3 km Positive Shear	3 X 10 ⁻³ s ⁻¹	10.3 X 10 ⁻³ s ⁻¹	10.3 X 10 ⁻³ s ⁻¹
0-3 km Bulk Shear	2 X 10 ⁻³ s ⁻¹	2 X 10 ⁻³ s ⁻¹	2 X 10 ⁻³ s ⁻¹
0-3 km SREH	150-250 m ² /s ²	139 m ² /s ²	164m ² /s ²
0-1 km SREH	~100 m ² /s ²	33m ² /s ²	19 m ² /s ²
0-1 km Positive Shear	> 10 X 10 ⁻³ s ⁻¹	10 X 10 ⁻³ s ⁻¹	10 X 10 ⁻³ s ⁻¹
0-1 km Bulk Shear	> 8 X 10 ⁻² s ⁻¹	8.8 X 10 ⁻³ s ⁻¹	8.8 X 10 ⁻³ s ⁻¹

Table 2. Kinematic parameters calculated from 1200 UTC hodographs created from KDDC (May 25) and KAMA (May 31) radiosonde data with comparative values from the refereed literature and “conventional wisdom.” The morning sounding and hodograph information is often the first information tornado researchers and storm chasers examine in assessing whether the kinematic environment is favorable for tornadic convection. Two right hand columns represent the values of the parameters assuming a forecast storm motion (using the Bunkers technique) and the actual storm motion. Color coding: Green (values equal or exceed those favorable); Yellow (values nearly equal to those favorable); and , Red (values do not meet minimum thresholds). Some shear values are given in knots because these are conventionally used in the field, and on SPC website displays. Positive shear values (defined in text) are included even though these are not commonly used in the field.

basis of the kinematic parameters shown for the morning hodographs is bad practice. For this reason, we have included the RUC13 hodographs for grid points closest to A1 (on Fig. 3) and C1 (on Fig. 4) at 1800 UTC for comparative purposes. The reader will note that the actual hodographs (at least, actual in terms of the RUC grid point hodographs) somewhat resembled the morning hodograph for the Campo case (Fig. 18b) but not at all for the Towner case (Fig. 17b). An interesting fact is that by 0000 UTC (Fig. 17c) the RUC13 hodograph for the Kiowa County area did indeed begin to resemble the hodograph in Fig. 17a, and by 0300 UTC resembled it quite closely.

The authors would also like to underscore an important point. Whether the hodographs that occurred in the storm initiation area (as estimated by the RUC13 hodographs shown in Figs. 17, b c and 18b) resembled the morning hodographs (and the judgments made on their bases) or not, the fact of the matter is that placing the actual storm motion into those hodographs too resulted in kinematic and wind shear parameters more favorable for storm ventilation and development of both mid level and low level rotation. In addition, use of bulk parameters (instead of, for example, positive shear) yielded values that would have underestimated the risk for tornadic convection for the wind environments shown by the RUC13 hodographs as well. Thus, the inaccurately forecast storm motion using conventional techniques resulted in an underassessment of the risk for long-lived, rotating, possibly tornadic storms.

4. CONCLUSIONS

Both the Kiowa County storm of 25 May and the Baca County storm of 31 May had life cycles and periods of evolution that had three phases. Phase 1 occurred near initiation time when strong convective updrafts interacted with the low level shear field augmented by boundaries to produce either non-mesocyclone (landspout) tornadoes or high-based funnel clouds.

In Phase 2, storms began to produce supercell tornadoes, but exhibited storm motions that deviated significantly from those expected using the Bunkers (or similar) techniques. Finally, in Phase 3, storms continued to produce mesocyclone-induced tornadoes, but storm motions resembled more closely those predicted by conventional techniques.

In this pilot study, the authors were interested in exploring why most forecasters (including forecasters from SPC and severe weather meteorologists out in the field assessing research or storm chase plans) underestimated the risk of afternoon tornadic convection on both days. For example, extracted from SPC's 1630 UTC 31 May convective outlook discussion for Day 1:

...SYNOPSIS...
GIVEN THE OVERALL WEAK SHEAR AND
SUBTLE BOUNDARIES IT IS DIFFICULT TO
DELINEATE REGIONS THAT WOULD BE
WORTHY OF MORE THAN LOW SEVERE
PROBABILITIES.

In this study, we have hypothesized why Phase 2 of the storm evolution on both days was largely unanticipated – a hypothesis that warrants further study in an expanded research effort resulting in a journal submission for this case. Another area of interest that the authors wish to explore is the fact that both of these storms were considered to be long-lived supercells. Recent research has been done on the topic of long-lived supercells, and we believe that these two cases could be considered outliers in the Bunkers dataset (Bunkers et al. 2006) based on the marginal middle tropospheric kinematic fields.

We maintain that there are important predictive issues for both of these cases. First, storm motions assessed from either the morning hodographs from the radiosonde sites closest to the storm initiation area OR the hodographs produced by the RUC in real time did not accurately resemble actual storm motions. This led to inaccurate assessment of storm-relative wind and wind shear parameters. Blind acceptance of the forecast storm motion, and the parameters that resulted from that, suggested that any storms that formed on these days would not be long-lived, and that the rotational parameters would not favor the development of sustained mid level rotation.

A second issue is that forecasters are accustomed to using indices and parameters that sometimes are based upon rules of thumb or common usage. We believe that the use of bulk shear values (instead of positive shear), for example, can misdirect forecaster attention from the significant geometry of the true wind profile (as analyzed on a hodograph) that could otherwise point to the possibility of supercell storms and strong low level mesocyclones leading to, perhaps, tornadogenesis, as is shown in both of the cases in this study.

Finally, we believe that our results show that boundaries played a very important role in the storm evolution on this day. It is true that many forecasters alluded to these boundaries (for example, the forecasters at SPC) as potentially important “players” on both days, but because the ground-relative wind shear and wind parameters were generally weak, it is easy to see that forecasters (both operationally and those out in the field conducting research and/or storm chasing) would have a lower level of concern for long-lived supercells producing numerous tornadoes.

5. ACKNOWLEDGEMENTS

Several storm chaser accounts, photograph, and videos were used to verify tornadoes in these cases, including those listed in Storm Data. Specifically, the authors would like to thank Robin Tanamachi, Howie Bluestein, and Nick Engerer for their detailed storm chase accounts on 25 May. The authors would like to thank Larry Ruthi, Meteorologist-in-Charge of National Weather Service, Dodge City, Kansas for his support in this research.

6. REFERENCES

Brown, R. A., L. R. Lemon, and D. W. Burgess, 1978: Tornado detection by pulsed Doppler radar. *Mon. Wea. Rev.*, **106**, 29-38.

Bunkers, M., Klimowski, J., Zeitler, J. W., Thompson, R. L., Weisman, M. L., 2000: Predicting supercell motion using a new hodograph technique. *Wea. Forecasting*, **15**, 61-79.

Bunkers, M. J., M. R. Hjelmfelt, and P. L. Smith, 2006: An observational examination of long-lived supercells. Part I: characteristics, evolution, and demise. *Wea. Forecasting*, **21**, 673-688.

---, J. M. Grzywacz, B. A. Klimowski, and M. R. Hjelmfelt, 2006: An observational examination of long-lived supercells. Part II: environmental conditions and forecasting. *Wea. Forecasting*, **21**, 689-714.

Markowski, P. M., E. N. Rasmussen, and J. M. Straka, 1998: The occurrence of tornadoes in supercells interacting with boundaries during VORTEX-95. *Wea. Forecasting*, **13**, 852-859.

Rasmussen, E. N., S. Richardson, J. M. Straka, P. M. Markowski, and D. O. Blanchard, 2000: The association of significant tornadoes with a baroclinic boundary on 2 June 1995. *Mon. Wea. Rev.*, **128**, 174-191.

Rotunno, R., and J. Klemp. 1985: On the rotation and propagation of simulated supercell thunderstorms. *J. Atmos. Sci.*, **42**, 271-292.

Thompson, R. and Edwards, R., 2000: An Overview of Environmental Conditions and Forecast Implications of the 3 May 1999 Tornado Outbreak. *Wea. Forecasting*, **15**, 682-699.

Weisman, M.L., and J.B. Klemp, 1982. The dependence of numerically-simulated convective storms on vertical wind shear and buoyancy. *Mon. Wea. Rev.*, **110**, 504-520.